Angle-resolved photoemission spectra from strong-coupling superconductors

G. V. Klimovich

Landau Institute for Theoretical Physics, Kosygina 2, 117334 Moscow, Russia

Angle-resolved photoemission from the normal and superconducting states is investigated both analytically and numerically in the model based on the strong-coupling theory of superconductivity. The results obtained are in good agreement with experimental data on high-resolution photoemission spectra of Bi-2212 compounds. The model gives a possible explanation of a number of unusual features of angle-resolved photoemission spectra from high-temperature superconductors.

1. INTRODUCTION

High-resolution photoemission spectra of high-temperature superconductors have revealed a number of distinctive features which can not be explained within the usual weak-coupling BCS theory of superconductivity. Among them is a dip appearing in angle-resolved photoemission spectra (ARPES) from the superconducting state, the position of the dip being at least approximately independent of photoemission angle.

Many attempts have been made to explain the emergence and behavior of such a dip from different points of view. In this article we present both analytical and numerical results which show that the dip and other properties of ARPES may be adequately described within the framework of the strong-coupling theory of superconductivity,[10] given a strong peak in the effective phonon density of states (PDOS).

In particular, it is shown that the usual (based on BCS) explanation of the peak in ARPES below E_F occurring in the superconducting state may be wrong, so an alternative treatment is proposed.

The outline of the article is as follows. In Sec. 2 we describe the model used. Section 3 discusses notation and mathematical details. In Sec. 4 we present computational results (along with analytical explanation) for ARPES taken in the normal ($T > T_c$) and superconducting ($T = 0$) states. Section 5 is about effects on ARPES of a gap anisotropy and strong electronic correlation which were not built into the model for computer simulations.

2. MODEL

Although the model for calculations is deliberately very simplified to reduce the number of model parameters to a minimum, it retains the essential physics related to the ARPES.

We will analyze a one-band metal with strong electron-phonon interaction; its electronic spectrum is quasi-two-dimensional in the plane parallel to the surface probed by the photoemission, so in calculations of ARPES the electron dispersion in the perpendicular direction may be neglected.

We will be interested in ARPES within a relatively narrow energy ($\lesssim 200$ meV from the Fermi level) and angular range, the emphasis being on the difference between ARPES in the normal and superconducting states. Therefore, we may disregard the details of the band structure, momentum and energy dependence of the matrix elements, and treat the ARPES intensity as being proportional to the spectral density of the single particle Green's function. Surface effects[1] will also be neglected.

Let the electronic spectrum $\xi_{\vec{p}} = \xi_{p_\parallel}$ be isotropic in the plane. In calculations we also disregard anisotropy of the order parameter Δ: $\Delta_{\vec{p}} = \Delta_{p_\parallel} \approx \Delta_{p_F}$.

To fit experimental results it is essential that the PDOS contain a strong peak; for simplicity we approximate the PDOS by the only peak at frequency $E = E_{ph} \approx 20$ meV whose half-width is $\gamma_{ph} \approx 10$ meV (see also Ref. 5). The constant of electron-phonon interaction is $\lambda = 4$. The computed critical temperature and gap at zero temperature are $T_c = 6.4$ meV $= 74$ K, and $\Delta_0 = 18$ meV respectively.

3. BASIC FORMULAE AND MATHEMATICAL DETAILS

The ARPES intensity is assumed to vary proportionally to the spectral density of the occupied states of the one-particle Green's function, the finite energy and momentum resolution being taken into account:

$$I(\varepsilon,\xi) = \int P_e(\varepsilon - \varepsilon') P_a(\xi - \xi')$$

$$\times \left(-\frac{1}{\pi} \operatorname{Im} G^R(\varepsilon',\xi') \right) d\varepsilon' d\xi', \tag{1}$$

where P_e is an energy resolution function, $\xi = \xi_{p_\parallel}$ is the electronic spectrum, P_a allows for angular resolution in terms of the ξ resolution, G^R is the retarded electron Green's function, and f is the Fermi distribution factor.

In the strong-coupling theory

$$G^R(\varepsilon,\xi) = \frac{Z\varepsilon + \xi}{Z^2(\varepsilon^2 - \Delta^2) - \xi^2}, \tag{2}$$

where $Z = Z(\varepsilon)$, $\Delta = \Delta(\varepsilon)$ are solutions of the Eliashberg equations.[10] They depend on the effective phonon density of states $g(E) = \alpha^2 F(E)$ (see notation in Ref. 3).

At zero temperature the gap in the spectrum Δ_0 is implicitly defined by the equation $\Delta_0 = \Delta(\varepsilon = \Delta_0)$. For our purpose it is convenient to adopt $g(E)$ in the following form:

$$g(E) = \frac{\lambda}{2\pi} \left(\frac{1}{(E - E_{ph})^2 + \gamma_{ph}^2} - \frac{1}{(E + E_{ph})^2 + \gamma_{ph}^2} \right) \frac{E_{ph}^2 + \gamma_{ph}^2}{E_{ph}} \gamma_{ph}, \quad (3)$$

matching the PDOS peak at $E \approx E_{ph}$ with half-width $\approx \gamma_{ph}$, and electron-phonon coupling constant

$$\lambda = 2 \int_0^\infty \frac{g(E)}{E} dE.$$

We use $E_{ph} = 20$ meV, $\gamma_{ph} = 10$ meV, and $\lambda = 4$, and obtain $\Delta_0 \approx 18$ meV and $T_c \approx 74$ K.

In (1) P_e is taken as a Gaussian,[5] while for P_a a Lorentzian is more convenient, since in the ARPES calculations the latter choice allows one to account for nonmagnetic impurities scattering just by enhancing the half-width γ_ξ of the Lorentzian, $\gamma_\xi \to \gamma_\xi + 1/2\tau_{imp}$:

$$P_e(\varepsilon - \varepsilon') = \frac{1}{\sqrt{2\pi}\sigma_\varepsilon} e^{-(\varepsilon - \varepsilon')^2 / 2\sigma_\varepsilon^2}, \quad (4)$$

$$P_a(\xi - \xi') = \frac{1}{\pi} \frac{\gamma_\xi}{\gamma_\xi^2 + (\xi - \xi')^2}. \quad (5)$$

If $A(-\varepsilon, \xi)$ denotes the spectral density subject to only angular smearing,

$$A(-\varepsilon, \xi) = \int P_a(\xi - \xi') \left(-\frac{1}{\pi} \text{Im } G^R(-\varepsilon, \xi') \right) d\xi'$$

$$= -\frac{1}{2\pi} \text{Im} \left(\frac{\frac{\varepsilon}{\sqrt{\varepsilon^2 - \Delta^2}} + 1}{Z\sqrt{\varepsilon^2 - \Delta^2} - \xi + i\gamma_\xi} - \frac{\frac{\varepsilon}{\sqrt{\varepsilon^2 - \Delta^2}} - 1}{Z\sqrt{\varepsilon^2 - \Delta^2} + \xi + i\gamma_\xi} \right), \quad (6)$$

then the photoemission intensity is

$$I(\varepsilon, \xi) = \int P_e(\varepsilon - \varepsilon') A(\varepsilon', \xi) f(\varepsilon') d\varepsilon'. \quad (7)$$

Sometimes we will use the following approximation for A in (7):

$$A(-\varepsilon, \xi) = -\frac{1}{\pi} \text{Im} \left(\frac{1}{Z\sqrt{\varepsilon^2 - \Delta^2} - \xi + i\gamma_\xi} \right) \Theta(\varepsilon - \Delta_0), \quad (8)$$

which proves to be correct at large ξ (see Sec. 4). For brevity we write

$$\xi_0(-\varepsilon) = Z\sqrt{\varepsilon^2 - \Delta^2}. \quad (9)$$

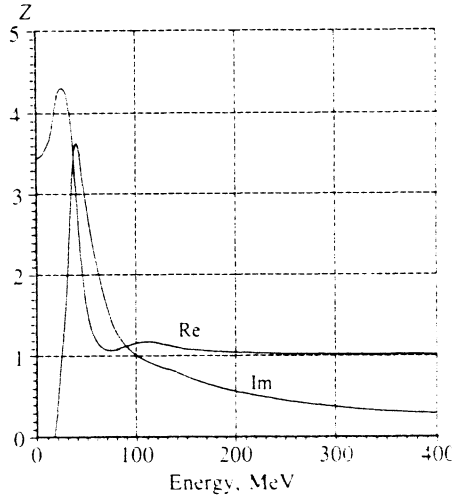All the numerical results for ARPES in the superconducting state are for zero temperature.

FIG. 1. The calculated dependence of $Z(\varepsilon)$ in the superconducting state at $T = 0$.

Since in the following section we exploit the qualitative behavior of $\xi_0(\varepsilon)$, the rest of this section outlines their analytical derivation in the strong-coupling theory.

For this purpose let us rewrite the Eliashberg equations at zero temperature in the following form, relating Z and Δ at real and Matsubara frequencies:[4]

$$(Z(\varepsilon) - 1)\varepsilon = \frac{1}{2} \int \lambda(\varepsilon - i\varepsilon_m) \frac{\varepsilon_m}{\sqrt{\Delta^2(i\varepsilon_m) + \varepsilon_m^2}}$$

$$+ \pi \int_0^\varepsilon g(\varepsilon - \varepsilon') \frac{\varepsilon'}{\sqrt{\Delta^2(\xi') - \varepsilon'^2}}; \quad (10)$$

$$Z\Delta(\varepsilon) = \frac{1}{2} \int \lambda(\varepsilon - i\varepsilon_m) \frac{\Delta(i\varepsilon_m)}{\sqrt{\Delta^2(i\varepsilon_m) + \varepsilon_m^2}}$$

$$+ \pi \int_0^\varepsilon g(\varepsilon - \varepsilon') \frac{\Delta(\varepsilon')}{\sqrt{\Delta^2(\varepsilon') - \varepsilon'^2}}. \quad (11)$$

For $\varepsilon > 0$, the principal value of the first integral in the r.h.s. is taken, the branch in the second integral is determined by the rule $\varepsilon' \to \varepsilon' + i0$:

$$\lambda(\zeta) = 2 \int_0^\infty \frac{g(E)E}{E^2 - \zeta^2} dE.$$

Figures 1 and 2 show the calculated Z and $\Delta(\varepsilon)$.

It may be shown that the behavior of Z, Δ at real frequencies is due to the superposition of singularities of both factors under the second integral in the r.h.s. In particular, a sharp peak in the PDOS at some energy E_{ph} with half-width γ_{ph} small in comparison with the gap value Δ_0, $\gamma_{ph} \ll \Delta_0$, leads to strong approximately equal singularities in $Z\varepsilon$, $Z\Delta$ at $\varepsilon = E_{ph} + \Delta_0$, which are also seen in the peaks of the real and imaginary parts of $\xi_0 = Z\sqrt{\varepsilon^2 - \Delta^2(\varepsilon)}$.
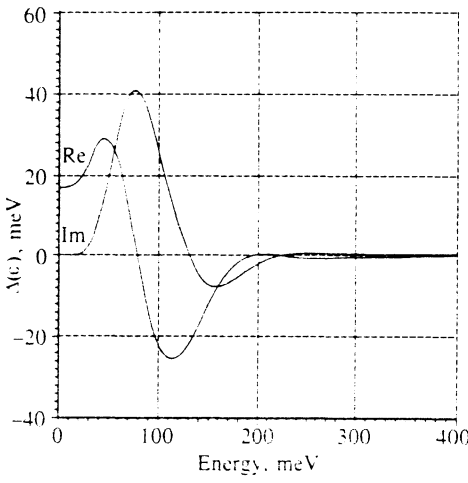
In our calculations the peak in the PDOS is not very sharp

FIG. 2. The calculated dependence of $\Delta(\varepsilon)$ in the superconducting state at $T=0$.

FIG. 4. ARPES calculated in the superconducting state ($T=0$) for $\xi=$ -100, -150, -200, -250 meV. (Resolution: $\sigma_\varepsilon=10$ meV, $\gamma_\xi=30$ meV.)

$$\gamma_{ph}=10 \text{ meV} \sim \Delta_0=18 \text{ meV},$$

but it still suffices to give peaks in

$$\text{Re,Im}[Z\sqrt{\varepsilon^2-\Delta^2(\varepsilon)}],$$

and also shows up in the nonmonotonic behavior of $\text{Re}[Z\sqrt{\varepsilon^2-\Delta^2(\varepsilon)}]$, as well as the sharp increase in $\text{Im}[Z\sqrt{\varepsilon^2-\Delta^2(\varepsilon)}]$ at $\varepsilon \approx E_{ph}+\Delta_0$—the properties we will use in the following Section.

4. RESULTS AND DISCUSSION

A. ARPES at large negative ξ

Figures 3 and 4 show computed ARPES from normal and superconducting states taken at *large negative* ξ, $|\xi| \gtrsim Z(\Delta_0+E_{ph})$. In agreement with the experiment (see Ref. 2 and references there), in the superconducting state a dip appears at around $\varepsilon = -65$ meV and an additional narrow peak at higher energies (the other low-energy peak
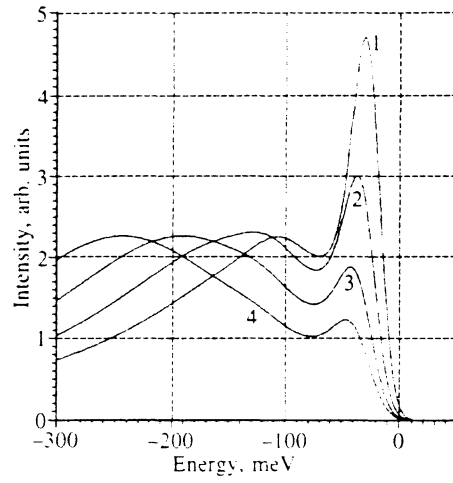
remains at $\varepsilon \approx \xi$). Such a picture can hardly be obtained in the BCS model under experimental energy resolution (as an example, see ARPES in Fig. 5 computed for the BCS model with the same gap at $T=0$—there is neither a dip nor an additional peak).

Strong-coupling theory turns out to be able to give a natural, though somewhat unexpected, explanation of the experimentally observed picture. For instance, let $\xi = -150$ meV. It can be shown that at large negative ξ we may use the approximate formula (8) to obtain the photoemission intensity from (7). Figure 6 shows $\text{Re,Im} \xi_0(-\varepsilon) = Z\sqrt{\varepsilon^2-\Delta^2}$. It is the nonmonotonicity of $\text{Re} \xi_0$ that suffices to cause the dip and additional peak of $A(\xi,-\varepsilon)$. Specifically, if $\text{Im} \xi_0$ were constant we would already expect from (8) a peak and dip in $A(\xi,-\varepsilon)$ at energies ε_1 and ε_2 of the maximum and minimum of $\text{Re} \xi_0$
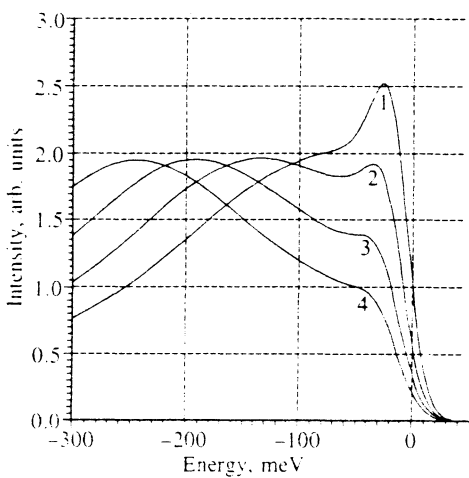

FIG. 3. ARPES calculated in the normal state ($T=75$ K) for $\xi=-100$, -150, -200, -250 meV. (Resolution: $\sigma_\varepsilon=10$ meV, $\gamma_\xi=30$ meV.)
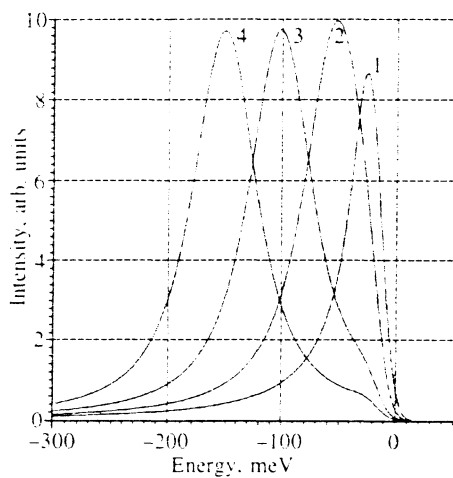

FIG. 5. ARPES calculated in the BCS approximation ($T=0$, $\Delta=18$ meV) for $\xi=0$, -50, -100, -150 meV. (Resolution: $\sigma_\varepsilon=10$ meV, $\gamma_\xi=30$ meV.)
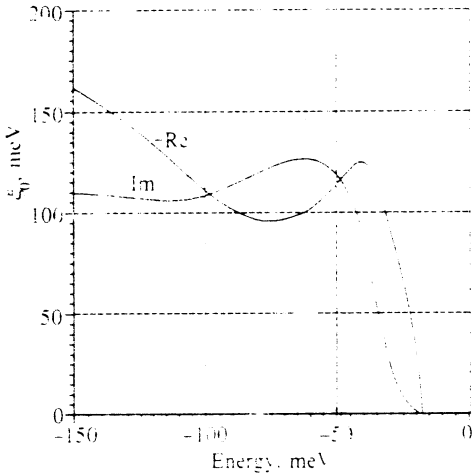
FIG. 6. The calculated dependence of Re, Im $\xi_0(-\varepsilon)$ in the superconducting state at $T=0$.

FIG. 8. ARPES calculated in the normal state ($T=75$ K) for $\xi=100$, 50, 0, -50 meV. (Resolution: $\sigma_\varepsilon=10$ meV, $\gamma_\xi=30$ meV.)

respectively. (Actually, the sharp increase in Im ξ_0 at $\varepsilon<\varepsilon_1$ further amplifies the dip value). These features of A manifest themselves in the photoemission intensity at sufficient energy resolution.

This qualitative dependence of Re, Im ξ_0 can be derived analytically in the strong-coupling theory (see Sec. 3). In the normal state (see Fig. 7) the corresponding dependence of $Z\varepsilon$ gets smoother, as expected. That is why the dip and additional peak almost or completely disappear (compare Fig. 4 with normal-state ARPES in Refs. 2, 6).

Now we will discuss the attempt to explain ARPES features in the framework of the BCS theory (the BCS approximation requires $Z(\varepsilon)\equiv1$, $\Delta(\varepsilon)\equiv\Delta_0$ in expression (2) for the electron Green's function).

From (6) we see that A has a square-root singularity at $\varepsilon=-\Delta_0$, so like A, the PE intensity can have peaks at $\varepsilon\sim-\Delta_0$, ξ, and a dip in between at large negative ξ. However, the singularity in A rapidly abates with ξ (as γ_ξ/ξ^2).

As a result, after reasonable energy resolution is taken into account the peak at $\varepsilon\sim-\Delta_0$ and the dip vanish. Moreover, this explanation fails at small negative and positive ξ in contradiction with the experimental data.

B. ARPES taken at ξ in the vicinity of the Fermi surface

Let us proceed to the treatment of ARPES calculated at nearly Fermi moment $|\xi|\lesssim Z(\Delta_0+E_{\text{ph}})$. The calculated spectra are presented on Figs. 8–12 (Figs. 11, 12 demonstrate the dependence of ARPES on energy and angular resolution, respectively). They may be compared with the experimental spectra in Refs. 2, 9. Again, our model correctly describes the appearance of the dip in the superconducting state, but the analytical explanation differs from that in the case of large negative ξ and may be ambiguous.
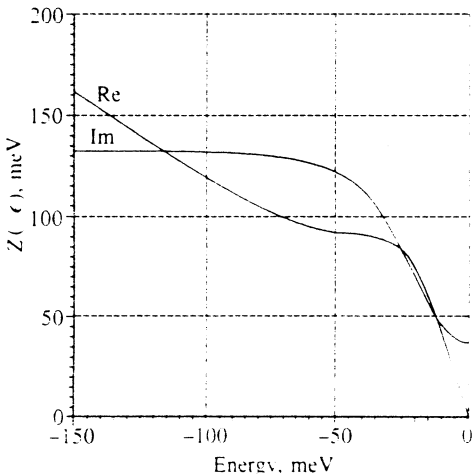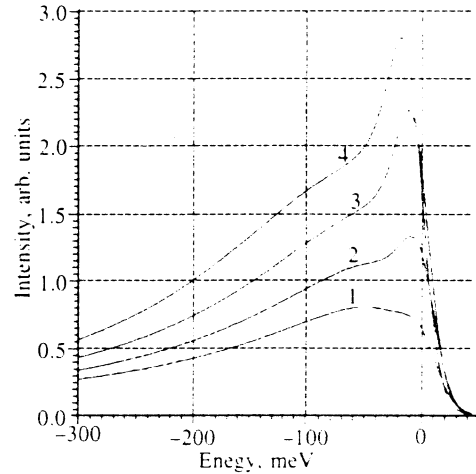

FIG. 7. The calculated dependence of Re, Im $Z(-\varepsilon)(-\varepsilon)$ in the normal state at $T=75$ K.
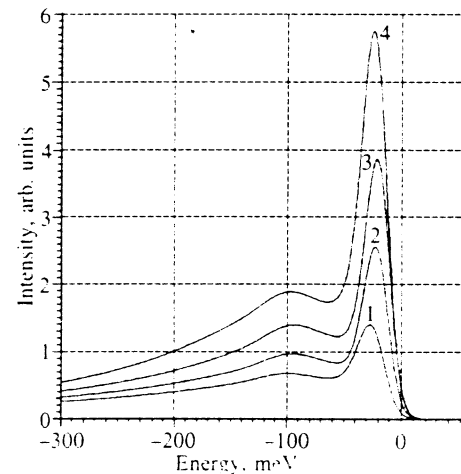

FIG. 9. ARPES calculated in the superconducting state ($T=0$) for $\xi=100$, 50, 0, -50 meV. (Resolution: $\sigma_\varepsilon=10$ meV, $\gamma_\xi=30$ meV.)
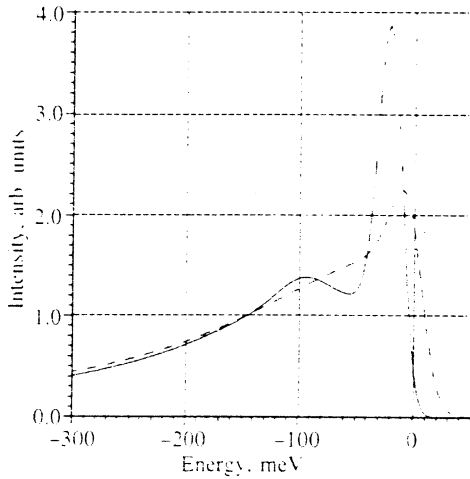
FIG. 10. ARPES calculated for $\xi=0$ in the normal (dashed line, $T=75$ K) and superconducting (solid line, $T=0$) states. (Resolution: $\sigma_\varepsilon=10$ meV, $\gamma_\xi=30$ meV.)
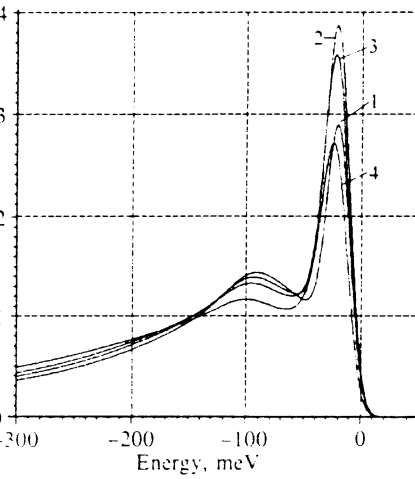
FIG. 12. Dependence of calculated ARPES in the superconducting state ($T=0$) on momentum resolution: $\gamma_\xi=10, 30, 50, 100$ meV, $\xi=0$, $\sigma_\varepsilon=10$ meV.
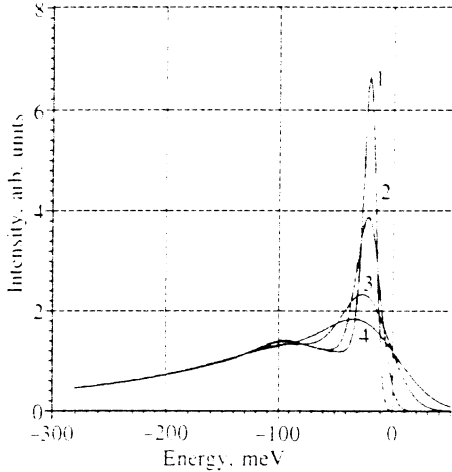
Let us first consider the case of perfect angular resolution ($\gamma_\xi=0$) for the $\xi=0$ spectrum. Then from (2,6,7) the photoemission intensity is

$$I(\varepsilon,\xi) = \int P_e(\varepsilon-\varepsilon')A(\varepsilon',\xi)f(\varepsilon')d\varepsilon', \qquad (12)$$

$$A(-\varepsilon,\xi) = -\frac{1}{\pi} \operatorname{Im} G^R(-\varepsilon,\xi) \qquad (13)$$

$$= -\frac{1}{\pi} \operatorname{Im}\left(\frac{Z\varepsilon+\xi}{Z^2(\varepsilon^2-\Delta^2)-\xi^2}\right). \qquad (14)$$

From the form of $Z(\varepsilon)$ and $\Delta(\varepsilon)$, $A(\varepsilon,0)$ has a singularity at $\varepsilon=-\Delta_0$, takes modest values at $\varepsilon<-\Delta_0$, $\varepsilon+(\Delta_0+E_{ph}) \gtrsim \gamma_{ph}$ in view of the small $\operatorname{Im} Z$, $\operatorname{Im} \Delta$, and reaches its maximum at some smaller ε. Such an $A(\varepsilon,0)$ manifests itself as a dip in $I(\varepsilon,0)$ for good energy resolu-

tion (see $I(\varepsilon,0)$ for $\gamma_\xi=10$ meV on Fig. 12). For a weaker angular resolution (Fig. 12, $\gamma_\xi=30$, 50 meV) it hardly explains the occurrence of the dip.

Finally, in the case of poor angular resolution the dip in ARPES at small ξ would naturally correspond to a minimum in the momentum-integrated electron density of states[5]

$$\nu(\varepsilon) = \operatorname{Re}\left(\frac{|\varepsilon|}{\sqrt{\varepsilon^2-\Delta^2}}\right)$$

(in Fig. 13 we picture part of the calculated $\nu(\varepsilon)$; it may be compared with $I(\varepsilon,0)$ for $\gamma_\xi=100$ meV in Fig. 12).

5. ADDITIONAL EFFECTS ON ARPES

The presented calculations were performed for an isotropic order parameter. On the other hand, there is exper-

FIG. 11. Dependence of calculated ARPES in the superconducting state ($T=0$) on energy resolution: $\sigma_\varepsilon=5, 10, 20, 30$ meV ($\xi=0$, $\gamma_\xi=30$ meV).
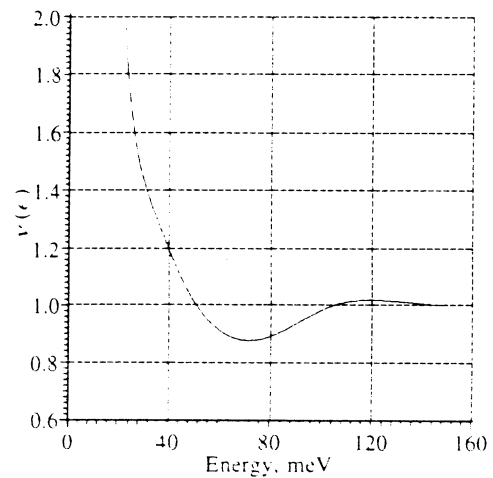
FIG. 13. Momentum-integrated density of states calculated in the superconducting state ($T=0$). (A narrow vicinity of the gap is not pictured.)

imental evidence[7] in favor of large gap anisotropy in Bi-2212 compounds, so we will consider how it affects ARPES. If we restrict ourselves to spectra taken parallel to the momentum when the gap size reaches its maximum, then the difference between ARPES in the normal and superconducting states is clearer.

We assume that strong-coupling theory remains in force, but the order parameter varies on the Fermi surface (FS): $\Delta = \Delta(\varepsilon, \vec{p})$ (say, due to the stronger momentum dependence of the electron interaction and the anisotropy of the electronic spectrum or difference in nature of FS constituents). Then we may use equations similar to (10) but with momentum-dependent Z and Δ and additional integration over the FS in the r.h.s.

Due to the variation of $\Delta(\vec{p})$ in the r.h.s., Z and Δ become smoother functions of energy in the superconducting state. As a result, some distinctive features of ARPES from the superconductor get less pronounced and can even disappear if the contribution of the FS regions with smaller gap sizes to the r.h.s. is large.

If strong electronic correlations are taken into account, the strong-coupling theory (with renormalized parameters) holds true in the frequency region close to the Fermi level,[11] while at lower frequencies one expects the appearance of a large background in ARPES due to the large imaginary part of the correlation self-energy of the electrons.

6. CONCLUSION

Using a simple model, we have shown how the behavior of ARPES from Bi-2212 compounds, such as the dip in the superconducting state, may be explained within the framework of the strong-coupling theory of superconductivity, if the effective phonon density of states has a pronounced peak at low ($E \sim 20$ meV) energies. Analytical evidence is presented along with the numerical results.

[1] A. Bansil et al., J. Phys. Chem. Solids **53**, 1541 (1992).
[2] D. S. Dessau et al., Phys. Rev. B **45**, 5095 (1992).
[3] J. P. Carbotte, Rev. Mod. Phys. **62**, 1027 (1990).
[4] E. Marsiglio, M. Schlossmann, J. P. Carbotte, Phys. Rev. B **37**, 4965 (1988).
[5] G. B. Arnold, F. M. Mueller, J. C. Swihart, Phys. Rev. Lett. **67**, 2569 (1991).
[6] Y. Hwu et al., Phys. Rev. Lett. **67**, 2573 (1991).
[7] Z.-X. Shen et al., Phys. Rev. Lett. **70**, 1553 (1993).
[8] C. G. Olson et al., Phys. Rev. B **42**, 381 (1990).
[9] D. S. Dessau et al., Phys. Rev. Lett. **66**, 2160 (1991).
[10] G. M. Éliashberg, Zh. Eksp. Teor. Phys. **39**, 1437 (1961) [Sov. Phys. JETP **12**, 1000 (1961)].
[11] G. M. Éliashberg, in Electronic Properties of High-Tc Superconductors, H. Kuzmany, M. Mehring, J. Fink (Eds.), Springer Series in Solid State Sciences, v. **113**, p. 385 (1993).

This article was published in English in the original Russian journal. It is reproduced here with stylistic changes by the Translation Editor.